2021 43rd Annual International Conference of the
IEEE Engineering in Medicine & Biology Society (EMBC)
Oct 31 - Nov 4, 2021. Virtual Conference

Short-training Algorithm for Online Brain-machine Interfaces Using One-photon Microendoscopic Calcium Imaging

Hung-Yun Lu[1], Anil Bollimunta[2], Ryan W. Eaton[3], John H. Morrison[3], Karen A. Moxon[3], Jose M. Carmena[4], Jonathan J. Nassi[2], Samantha R. Santacruz[1*]

Abstract— **Calcium imaging has great potential to be applied to online brain-machine interfaces (BMIs). As opposed to two-photon imaging settings, a one-photon microendoscopic imaging device can be chronically implanted and is subject to little motion artifacts. Traditionally, one-photon microendoscopic calcium imaging data are processed using the constrained nonnegative matrix factorization (CNMFe) algorithm, but this batched processing algorithm cannot be applied in real-time. An online analysis of calcium imaging data algorithm (or OnACIDe) has been proposed, but OnACIDe updates the neural components by repeatedly performing neuron identification frame-by-frame, which may decelerate the update speed if applying to online BMIs. For BMI applications, the ability to track a stable population of neurons in real-time has a higher priority over accurately identifying all the neurons in the field of view. By leveraging the fact that 1) microendoscopic recordings are rather stable with little motion artifacts and 2) the number of neurons identified in a short training period is sufficient for potential online BMI tasks such as cursor movements, we proposed the short-training CNMFe algorithm (stCNMFe) that skips motion correction and neuron identification processes to enable a more efficient BMI training program in a one-photon microendoscopic setting.**

I. Introduction

Brain-machine interface (BMI) is a cutting-edge technique that enables communication between humans and their surroundings. By recording and decoding the brain signals, BMIs can restore lost physical movements, recognize speech patterns, and enhance vision and hearing. As a bridge between the brain and neuroprosthetic devices, BMIs rely on decoding algorithm to learn and interpret the recorded signals. Electrophysiology techniques are typically used to record action potentials ("spikes") in BMI paradigms. Despite the prevalence of use in BMI decoders, however, electrophysiological recordings have several limitations [1]. First, the neural activity is sparsely sampled and the number of isolated neurons is typically limited to the number of electrode contacts. Second, the recorded spikes can be prone to signal contamination by neighboring neurons. This problem is even exaggerated if the brain region of interest is structured with densely packed cells. Third, the spiking data provide little information about cellular identity. Even though waveforms of spikes can be used to give some confidence in uniqueness of identity and perhaps basic cell-type classification, such as excitatory versus inhibitory neurons, it is still not capable of informing with certainty the identity of neurons and physiological details of recorded units. Moreover, spiking data cannot provide spatial profiles of the region of interest even with the help of a stereotaxic instrument. These drawbacks have emphasized the importance of techniques other than electrophysiology.

Calcium imaging, an alternative optogenetic technique, is a powerful tool to optically interrogate neural activity at cellular and subcellular levels. Supported by the development of transfection techniques, calcium imaging can selectively image over an entire population of neurons with clear contours of microstructures and can longitudinally track individual neurons over time. Two-photon calcium imaging has rendered fruitful research outcomes in both rodents and non-human primates (NHP) [2], [3]. Despite its power, the study of BMIs using calcium imaging is still in its infancy [4], [5]. To date, two-photon calcium imaging data was successfully leveraged to decode movement direction in NHPs such as marmosets [6] and even rhesus macaques [7].

However, two-photon calcium imaging suffers from several disadvantages [8], including (1) higher infection risks during implantation and throughout experiments, (2) the daily manual alignments of the microscope for a consistent field of view, and (3) the physical constraint to the subject's brain. Most of these disadvantages can be easily resolved by replacing the two-photon microscope with a miniature one-photon microscope. The nVista (Inscopix, Inc., Palo Alto, CA) is a light-weight microscope which can be easily attached to a chronically implanted microendoscopic probe. This one-photon microendoscopic setting provides a much lower risk of infection and is compatible with the subject freely behaving without head restraint. Since the device is chronically implanted, the daily alignment procedure can also be bypassed. Therefore, one-photon microendoscopic calcium imaging holds great potential to be applied to BMIs, but this important research topic has not yet been explored. We implanted a gradient-refractive index (GRIN) lens in the dorsal premotor cortex of a rhesus macaque's brain that can image deeper cortical tissue and connect with a miniature microscope [8]. Here, we process the one-photon microendoscopic calcium imaging data with our proposed stCNMFe algorithm. We report the preliminary performance of stCNMFe by comparing the neuronal identification results with CNMFe. This research

[1]H.-Y. Lu and S.R. Santacruz are with the Biomedical Engineering department at University of Texas at Austin; Austin, TX, USA.

[2]A. Bollimunta and J.J. Nassi are with Inscopix, Inc.; Palo Alto, CA, USA.

[3]J. Morrison, and K.A. Moxon are, and R.W. Eaton was previously with California National Primate Research Center; Davis, CA, USA, and University of California, Davis; Davis, CA, USA.

[4]J.M. Carmena is with the Electrical Engineering & Computer Sciences department and the Helen Wills Neuroscience Institute at University of California, Berkeley; Berkeley, CA, USA

This work is supported by CNPRC Pilot Grant Program, P51-OD011107.

* s.santacruz@austin.utexas.edu

is a cornerstone for applying one-photon microendoscopic calcium imaging to BMIs.

II. Materials and Methods

A. Experimental Subjects

The rhesus macaques were obtained from the California National Primate Research Center (CNPRC) at UC Davis. The study used two healthy adult male monkeys at 5-8 years of age and weighing 13-14 kg. Animals were housed at the CNPRC at UC Davis. All experiments were conducted in compliance with the NIH Guide for the Care and Use of Laboratory Animals and were approved by the Institutional Care and Use Committee at the University of California, Davis.

B. Microendoscopic calcium imaging

To enable calcium imaging using a microendoscopic one-photon microscope in a behaving rhesus macaque, we injected a virus to the brain in order to express GCaMP and chronically implanted a microendoscopic gradient-refractive index lens for the microscope to access the same region as the injected virus. We used two different adeno-associated viral (AAV) strategies for expressing GCaMP. The first one was the conventional AAV (AAV1.CaMK2a.GCaMP6f) that was proven effective for GCaMP-based two-photon calcium imaging in macaque models [9]. The second one was an AAV Tet-Off viral system, which includes the mixture of an tetracycline transactivator (tTA) protein (AAV5.Thy1s.tTA) and a tetracycline responsive GCaMP component (AAV5.TRE3.GCaMP6f) [10]. The Tet-Off system resulted in higher levels of expression as compared to the conventional virus and can be temporarily suppressed by the administration of tetracycline or its derivatives, such as doxycycline.

The GRIN prism lens (1 mm diameter, 9 mm length Proview Integrated Prism Lens; Inscopix, Inc.) was inserted to 2 mm below the cortical surface after a linear incision in the targeted cortex. A side-view imaging plane was then attached to the end of the lens, and an integrated microscope baseplate was securely attached as a docking station for the miniature microscope. The final lens implants were secured with a customized cranial chamber with a removable cap and were completely sealed with cement and acrylic, minimizing the risk of infection and the effort of maintenance.

Beginning two weeks following the lens implantation surgery, calcium imaging was performed in the awake and behaving macaque, typically multiple times per week. The animal sat comfortably in a standard primate chair and was restrained temporarily to remove the chamber cap in order to plug in the miniature microscope and the data acquisition system. After the cap was removed, the baseplate is clearly and easily revealed so the miniature microscope can be docked to the station with a single screw. The animal was then placed in a chair with neck plates and the calcium imaging initiated. During the imaging sessions, the animal was completely free to behave without head restraint, including reaching, directing the positions of the head, and chewing.

C. Short-training CNMFe

To infer neural activity from calcium imaging data, a constrained nonnegative matrix factorization (CNMF [11], or CNMFe [12] for microendoscopic settings) method is commonly used. CNMFe can simultaneously identify the source of neurons, separate spatially overlapping components, denoise, and deconvolve the spiking activity. The spatiotemporal calcium dynamics can be seen as the product of two matrices: one that represents the location of the neurons, and the other that characterizes the temporal dynamics of corresponding neurons. Unlike traditional Independent Component Analysis approach, a nonlinear method such as nonnegative matrix factorization can better recognize overlapping components in space. By analyzing the calcium dynamics with CNMFe, we can obtain the estimated contours for all neurons identified by CNMFe and the corresponding fluorescent traces, which can further be correlated with other experimental setup such as eye saccade or hand movements.

The CNMFe algorithm can be streamlined into four separate steps, including spatial filtering, motion correction, source extraction, and an optional deconvolution process. For one-photon microendoscopic calcium images, the spatial filtering is essential because the images are not optically focused to a thin plane as specialized in two-photon imaging. The spatial filtering can effectively reveal the spatial features that are candidates for neurons. The motion correction relies on the NoRMCorre algorithm that corrects non-rigid motion artifacts by splitting the field of views into overlapping patches and then merging by smooth interpolation after registering separately [13]. In the source extraction step, each source of neurons can be seen as a product of two matrices: one that describes the spatial footprints of the source and the other that describes the temporal traces over time. Typically, the CNMFe framework can be mathematically described as Equation (1), where $Y \in R^{d*T}$ is a matrix that represents the observed data: d is all the observed pixels, and T is the number of time points (frames). $A \in R^{d*N}$ is the spatial information of the N neurons in the field of view, and $C \in R^{N*T}$ is the temporal profile of corresponding neurons. B represents the background fluctuation and E is the noise term.

$$Y = AC + B + E \tag{1}$$

Our goal is to find the matrices A and C by minimizing the Frobenius form of residual sum of squares (Eq. 2) with some constraints to A, B, and C. The matrices A and C are nonnegative because of the physical properties of these variables. It is also common to enforce sparsity constraints by penalizing the norms of spike counts matrices [11]. Constraints on the matrix B marks the main difference between CNMF and CNMFe. Instead of modeling B as a rank-1 nonnegative matrix, CNMFe decomposes the background fluctuation into two separate terms: fluctuating activity and constant baselines [12].

$$\|Y - (AC + B)\|_F^2 \tag{2}$$

As a batched processing method, CNMFe requires access to the entire set of data for processing. In order to enable frame-by-frame online operation, stCNMFe is proposed in this study. We used a brief snippet of imaging data taken from the beginning of recording session, usually between thirty seconds and two minutes in length, as short training dataset for CNMFe. The cellular contours are identified and used as the templates for fluorescence intensity extraction in the testing phases (the remainder of the imaging recording session). In the test dataset, we skip the redundant cellular identification process and the motion correction process due to the stability of the implant.

Since we use less data for training, it is expected that some neurons are not initially identified by this model. However, this cost comes with the gain of rapid, online detection of a stable population of neurons. We hypothesized that the stable recordings can guarantee sufficiently reliable identification results to enable online BMIs.

III. Results

For this work, we present results from five representative sessions of recorded calcium imaging data (612±66 second, mean ± std) that was acquired at 20 frames per second over three separate days. Each session is preprocessed by spatial and temporal downsampling followed by a bandpass spatial filter.

We first characterized the performance of CNMFe on these data by determining the cellular contours of neurons identified by CNMFe and the corresponding fluorescence traces over time in four example neurons (Fig. 1). The background in Figure 1(a) is the max-correlation image where the value for each pixel represents the correlation between the pixel and its eight neighbors. It is calculated for each 1000 frames across time and then the maximum correlation of that pixel will be taken. This method enhances the active neurons while suppressing background fluctuation and noises [14].

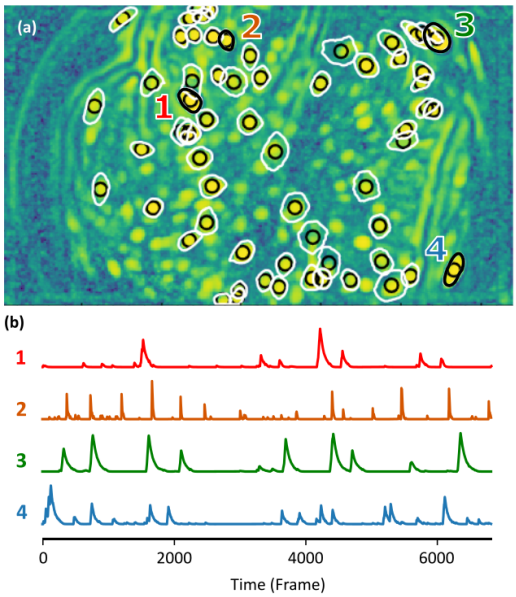

Figure 1. Representative performance of CNMFe. The white contours in (a) represents the identified neurons and the black circles are the center of mass. The traces in (b) represent the normalized fluorescence intensities across time in four example neurons labeled in (a).

We visualized the cellular contours of each identified cell in an example stCNMFe (Fig. 2a, stCNMFe trained by a 1.5-minute video) and CNMFe (Fig. 2b) models. Red contours in both figures are mutually identified, and the black contours are either false positive (Fig. 2a) or false negative (Fig. 2b). The fluorescence traces of one example neuron pointed by the blue and red triangles are shown in Figure 3. The upper figure showed the normalized fluorescence intensity of that neuron captured by stCNMFe and CNMFe, and the bottom figure showed the absolute difference between the two traces (Fig. 3). In this specific example, the trace from stCNMFe resembles the one from CNMFe, indicating the contour is nearly identically depicted by both models. It also confirms the stability of the microendoscopic implant, proving that motion correction is not required in this setting. The blue trace only has minor fluctuation in the testing phase due to the micromovement of the brain. However, the overall calcium dynamics of this neuron had been successfully captured by a training set that lasted for only 90 seconds. These results support our hypothesis that training on a short video may be sufficient to extract cellular components and corresponding neural activities for a BMI decoder.

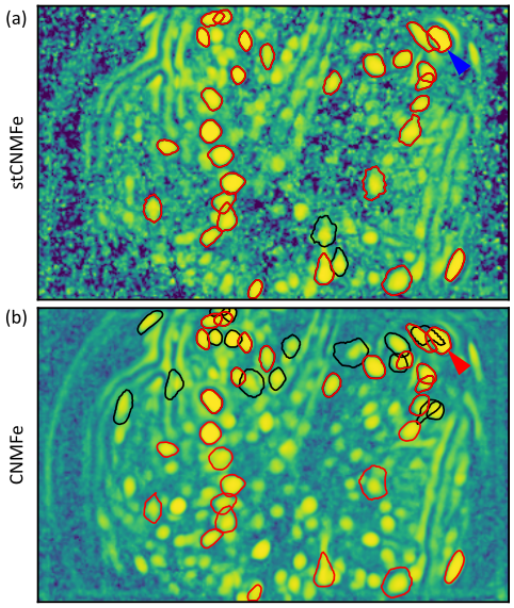

Figure 2. Example contours identified by (a) stCNMFe and (b) CNMFe. Both models are trained by the same recording session, except the stCNMFe is trained by the first 90 seconds of data. Red contours are mutually identified cells.

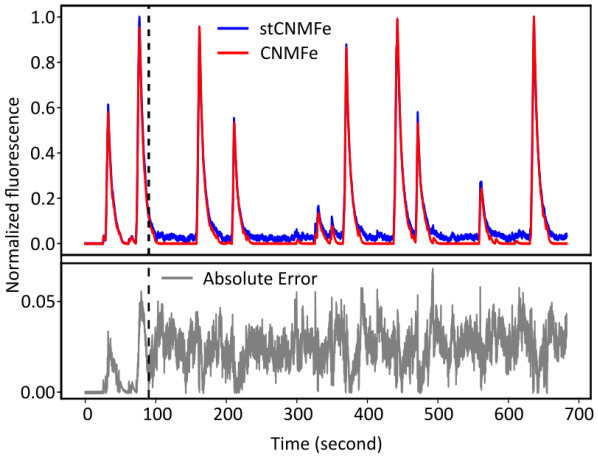

Figure 3. Normalized fluorescence traces of the labeled cell in Fig. 2 by stCNMFe and CNMFe. The dashed line marks the end of training phase.

Next, we benchmarked the identification efficacy and accuracy of stCNMFe as a function of the length of short-training videos (Fig. 4). The identification efficacy is defined as the number of neurons identified by stCNMFe divided by the number identified by CNMFe based on the whole batch of data. It represents how effective the stCNMFe model can extract neurons from a short video. The identification accuracy,

on the other hand, is the number of cells mutually identified by stCNMFe and CNMFe, which describes how accurate this model can identify the true labels. The stCNMFe model trained using only two-minute videos can identify more than 46% of the cells accurately (N = 22.6 neurons, the orange bar of 120 seconds in Fig. 4), while the stCNMFe models trained by only one-minute videos can still correctly locate 31% of the cells (N = 15.0 neurons, the orange bar of 60 seconds in Fig. 4) on average. BMIs using electrophysiology recordings in NHPs typically use cells as few as 15, and as many as 100 or more [4], [15], [16], demonstrating the potential of our method to sufficiently identify populations of neurons that can be used in online BMIs. We also evaluate the identification efficiency as the number of neurons identified divided by the time for training (Fig. 5). These results show that stCNMFe is significantly more efficient than CNMFe when using one to two minutes of training videos ($F_{4,20}=7.79$, $p<0.001$; one-way ANOVA, post-hoc Tukey's honest significance difference (HSD) test).

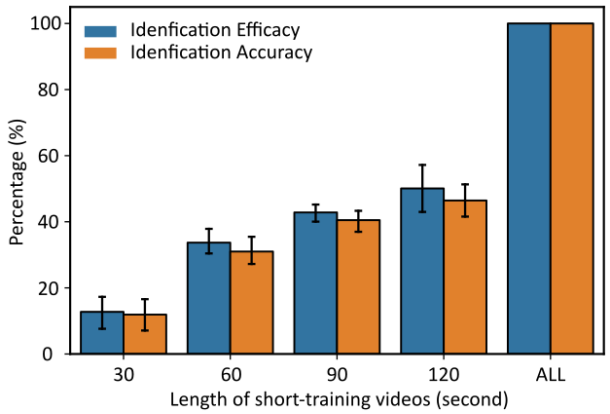

Figure 4. Identification efficacy and accuracy of stCNMFe as a function of the length of short-training videos. "ALL" represents training on the entire video (a.k.a. CNMFe). Error bars for all figures are standard deviations.

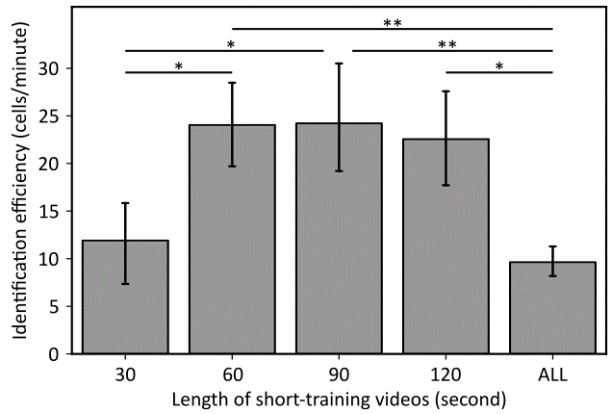

Figure 5. Identification efficiency of stCNMFe as a function of the length of short-training videos. Significant differences are shown as follows: *p < 0.05, **p < 0.01, and not significant if not indicated.

Conclusion

This study demonstrates the concept that one-photon micro-endoscopic calcium imaging data have the potential to be applied to online BMIs. By using stCNMFe, neurons can be effectively and efficiently identified compared to traditional CNMFe. For further exploration, our results suggested that only a short-training session is required for a BMI task. Although the model may not identify every neuron in the field of view, it does identify a large portion of neurons matching or exceeding the number necessary for BMIs and can do so in real-time.

References

[1] K. D. Harris, R. Q. Quiroga, J. Freeman, and S. L. Smith, "Improving data quality in neuronal population recordings," *Nat. Neurosci.*, vol. 19, no. 9, pp. 1165–1174, Sep. 2016, doi: 10.1038/nn.4365.

[2] S. L. Macknik *et al.*, "Advanced Circuit and Cellular Imaging Methods in Nonhuman Primates," *J. Neurosci.*, vol. 39, no. 42, p. 8267, Oct. 2019, doi: 10.1523/JNEUROSCI.1168-19.2019.

[3] J. L. Chen, M. L. Andermann, T. Keck, N.-L. Xu, and Y. Ziv, "Imaging Neuronal Populations in Behaving Rodents: Paradigms for Studying Neural Circuits Underlying Behavior in the Mammalian Cortex," *J. Neurosci.*, vol. 33, no. 45, p. 17631, Nov. 2013, doi: 10.1523/JNEUROSCI.3255-13.2013.

[4] D. J. O'Shea *et al.*, "The need for calcium imaging in nonhuman primates: New motor neuroscience and brain-machine interfaces," *Bio-Electron. Prosthet. Neurol. Dis.*, vol. 287, pp. 437–451, Jan. 2017, doi: 10.1016/j.expneurol.2016.08.003.

[5] K. B. Clancy, A. C. Koralek, R. M. Costa, D. E. Feldman, and J. M. Carmena, "Volitional modulation of optically recorded calcium signals during neuroprosthetic learning," *Nat. Neurosci.*, vol. 17, no. 6, pp. 807–809, Jun. 2014, doi: 10.1038/nn.3712.

[6] T. Ebina *et al.*, "Two-photon imaging of neuronal activity in motor cortex of marmosets during upper-limb movement tasks," *Nat. Commun.*, vol. 9, no. 1, pp. 1–16, May 2018, doi: 10.1038/s41467-018-04286-6.

[7] E. Trautmann *et al.*, "Dendritic calcium signals in rhesus macaque motor cortex drive an optical brain-computer interface," *bioRxiv*, p. 780486, Jan. 2019, doi: 10.1101/780486.

[8] A. Bollimunta* and S. R. Santacruz* *et al.*, "Head-mounted microendoscopic calcium imaging in dorsal premotor cortex of behaving rhesus macaque," *bioRxiv*, p. 2020.04.10.996116, Jan. 2020, doi: 10.1101/2020.04.10.996116.

[9] M. Li, F. Liu, H. Jiang, T. S. Lee, and S. Tang, "Long-Term Two-Photon Imaging in Awake Macaque Monkey," *Neuron*, vol. 93, no. 5, pp. 1049-1057.e3, Mar. 2017, doi: 10.1016/j.neuron.2017.01.027.

[10] O. Sadakane *et al.*, "Long-Term Two-Photon Calcium Imaging of Neuronal Populations with Subcellular Resolution in Adult Non-human Primates," *Cell Rep.*, vol. 13, no. 9, pp. 1989–1999, Dec. 2015, doi: 10.1016/j.celrep.2015.10.050.

[11] E. A. Pnevmatikakis *et al.*, "Simultaneous Denoising, Deconvolution, and Demixing of Calcium Imaging Data," *Neuron*, vol. 89, no. 2, pp. 285–299, Jan. 2016, doi: 10.1016/j.neuron.2015.11.037.

[12] P. Zhou *et al.*, "Efficient and accurate extraction of in vivo calcium signals from microendoscopic video data," *eLife*, vol. 7, p. e28728, Feb. 2018, doi: 10.7554/eLife.28728.

[13] E. A. Pnevmatikakis and A. Giovannucci, "NoRMCorre: An online algorithm for piecewise rigid motion correction of calcium imaging data," *J. Neurosci. Methods*, vol. 291, pp. 83–94, Nov. 2017, doi: 10.1016/j.jneumeth.2017.07.031.

[14] A. Giovannucci *et al.*, "CaImAn an open source tool for scalable calcium imaging data analysis," *eLife*, vol. 8, p. e38173, Jan. 2019, doi: 10.7554/eLife.38173.

[15] J. M. Carmena *et al.*, "Learning to Control a Brain–Machine Interface for Reaching and Grasping by Primates," *PLOS Biol.*, vol. 1, no. 2, p. e42, Oct. 2003, doi: 10.1371/journal.pbio.0000042.

[16] K. Ganguly and J. M. Carmena, "Emergence of a Stable Cortical Map for Neuroprosthetic Control," *PLOS Biol.*, vol. 7, no. 7, p. e1000153, Jul. 2009, doi: 10.1371/journal.pbio.1000153.